

# Bio-inspired Solar Desalination with Zero Liquid Discharge

C. Finnerty\* and B. Mi\*

\*Department of Civil & Environmental Engineering, University of California, Berkeley, California 94720, United States, casey.finnerty@berkeley.edu, mib@berkeley.edu

## ABSTRACT

To address the global rise of water demand, new approaches for desalination need to be developed. Solar steam generation is an emerging technique that utilizes sunlight to efficiently vaporize water and separate it from salts in solution. Although materials used to facilitate solar desalination show great promise, there are still some technical challenges that need further investigation. Two of these challenges include (1) understanding the limits and potential of passive water transport from the bulk solution to the steam-generating material and (2) characterizing the effects and salt crystal formation on performance. This paper evaluates these technical aspects using a graphene oxide (GO)-based steam-generating material (GO leaf). The solar desalination setup for the GO leaf has a unique water transport system that decouples insulation and water supply, freeing the steam-generating material from the floating configuration that is commonly used. Preliminary models for water transport have been developed to understand how a water lifting system can operate passively, through processes such as capillary action. Furthermore, the ability to control the direction of salt crystal formation was tested on the GO leaf to evaluate some positive implications of scaling. This investigation further elucidates the potential of solar steam generation for desalination and demonstrates the applicability of this technology as a energy-sustainable approach for zero liquid discharge.

**Keywords:** solar steam generation, heat localization, desalination, zero liquid discharge, graphene oxide

## 1 INTRODUCTION

### 1.1 Energy Consumption of Desalination

Over the past few decades, major advancements have dramatically reduced the energy consumption of desalination technologies. For example, a state-of-the-art reverse osmosis (RO) membrane system operating on seawater with a recovery rate of 50% only consumes 2 kWh/m<sup>3</sup>, which is only 25% higher than what is practically feasible from a seawater desalination plant [1]. This is because the energy required for desalination is fundamentally linked with water salinity. So even if that seawater desalination plant were able to operate at its

thermodynamic limit (1.06 kWh/m<sup>3</sup>), RO is still considerably more energy intensive than conventional water treatment (0.36 kWh/m<sup>3</sup>) [2], wastewater recycle (0.70 kWh/m<sup>3</sup>) [3], and sometimes importing water (1.10 kWh/m<sup>3</sup>) [4]. Energy intensity only becomes more of a problem in high salinity applications, such as zero liquid discharge. Concentrating saline water until the salt crystallizes requires mechanical vapor compression (MVC)-based brine concentrators and crystallizers, which consume 20-25 kWh/m<sup>3</sup> and 52-66 kWh/m<sup>3</sup>, respectively [5].

### 1.2 Steam-Generating Materials

Steam-generating materials have recently gained attention for their ability to convert light into heat, which can then be directly used towards vaporizing water. Although there has been a lot of work on the development of various light-absorbing materials [6 - 10], the primary characteristics required of these materials are (1) broadband light absorption, (2) heat localization, and (3) adequate water supply for replenishment. As the development of steam generating materials continues to mature, the focus has begun to shift away from developing ideal light absorbing materials toward some of the more practical challenges associated with this emerging technology. Two primary challenges include: (1) limited surface area for steam generation and (2) degraded performance when operating on saline water sources. The limited surface area for steam generation is often a product of how water is transported to the steam-generating surface. Relying on capillary action to replenish the water that has been vaporized from the pores of the steam generating material, these materials are often floated on the water's surface. However, the water in direct contact with the steam-generating material can act as a heat sink, drawing away heat that would otherwise be used for vaporizing water. Although some work has been done to insulate the steam-generating material from the water [11 - 12], the pathways of water transport through the insulation become coupled with parasitic heat loss to the water body and the overall rate of water evaporation becomes limited (i.e. higher evaporation rates require larger water channels, which results in greater heat loss). Furthermore, the amount of area for steam generation is also limited by the available surface area of the water body, necessitating large areas of land use to achieve comparable water production rates to those of other competing technologies.

The degraded performance when operating on saline water is often attributed to the formation of salt crystals on the surface of the steam generating material. Although some work has been done on how to redissolve [13] or precipitate this salt elsewhere [14], using the salt crystals to enhance performance has not been investigated.

### 1.3 Bio-Inspired Design

In nature, the trees are capable of lifting water great distances through transpiration [15]. Using vapor pressure gradients to drive this process, trees initiate transpiration by opening stomatal pores in the leaves. Evaporation out of capillaries in the intercellular space of the leaf creates a negative pressure in the xylem of the tree, which—in combination with capillary action—prompts water to travel from the soil into the tree’s roots. In order to generate enough negative pressure to facilitate transpiration, trees need large areas over which evaporation can take place. This brings in the idea of leaf area index (LAI) or the amount of leaf area with respect to the amount of land area taken up by the tree [16]. If solar desalination technologies could incorporate LAI values comparable to trees, the water production rate could increase 2 to 5 times [17].

Nature also provides instances of natural desalination. Specifically, the mangrove tree has a complex salt management process that enables it to thrive in waters exceeding the salinity of seawater [18]. Powered by the same mechanism as transpiration, the mangrove tree has filtering structures in its roots, allowing for the substantial rejection of salt. When excess salt passes through the root, the mangrove is able to isolate and excrete salt out of designated pores on the leaf’s surface [19]. By mimicking the mangrove tree’s ability to direct salt crystal formation, solar desalination technologies could potentially mitigate negative effects of operating on saline waters.

This paper describes some initial work in incorporating LAI and directed salt crystal formation into solar desalination by studying some of the underlining factors that influence these processes.

## 2 MATERIALS & METHODS

### 2.1 GO Leaf Synthesis

The solar steam generating material was synthesized by cross-linking GO nanosheets with triethylenetetramine (TETA) and 1,4-butanediol diglycidyl ether (BDGE) [20] onto a cellulosic substrate. This was accomplished by mixing these chemical precursors on ice at high pH. Once the solution had been well mixed, it was used to soak a coupon of Whatman filter paper. The soaked filter paper was immediately flash frozen using liquid nitrogen and placed in a freeze drier operating at  $-50^{\circ}\text{C}$  and pressures less than 0.2 mbar. The coupon was then transferred to a  $100^{\circ}\text{C}$  oven to cure. After rinsing several times with water, the steam-generating material (GO leaf) was synthesized.

### 2.2 Decoupled Water Transport & Insulation

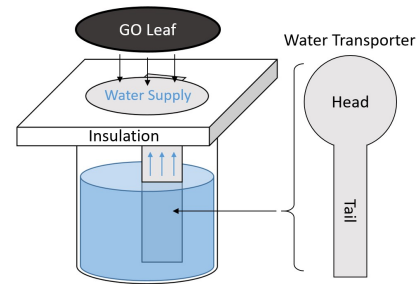


Figure 1: Decoupled water transport setup.

The setup used to evaluate steam generation performance lifts water from a bulk solution to the steam-generating material (see Fig. 1). The material used to transport water is an absorbent polystyrene sheet that relies on capillary forces to deliver water to the GO leaf. The head of the water transporter rests on a piece of insulating styrofoam and is sandwiched by the GO Leaf to ensure efficient water conveyance. Modifications of this setup include cutting the polystyrene sheet to make three additional tails for water transport and using an aluminum seal tape to reduce light penetration through the styrofoam and create better contact between the water transporter and the GO leaf. Using the polystyrene sheets for water transport and the styrofoam for insulation, this setup enables the GO leaf to be lifted from the water surface. When comparing the area of water transport to the area of the GO leaf, this setup operates at an LAI equivalent to 8.18.

### 2.3 Performance Evaluation

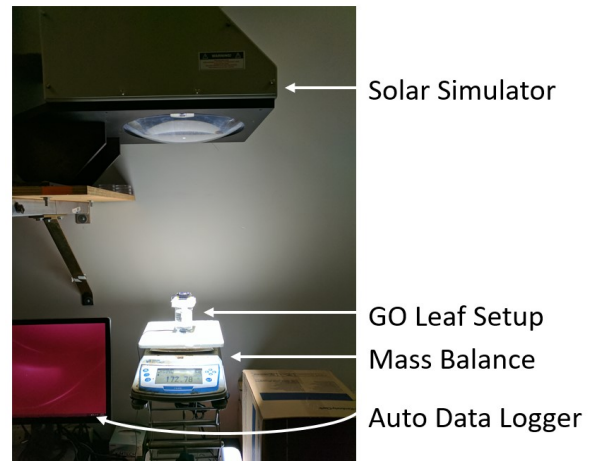


Figure 2: Equipment used for evaluating solar steam-generating performance.

Performance was evaluated by irradiating the steam-generating material with simulated sunlight ( $1,000 \text{ W/m}^2$ ) and recording the change in mass over time (see Fig. 2). By

normalizing this to the area of the steam-generating material, the evaporation flux may be determined. To evaluate the effects of water transport, the evaporation rate was monitored when operating with deionized water at two different distances from the GO leaf: 3.5 cm and 10 cm. To evaluate the ability to direct salt crystal formation, the feed solution was changed to 5 M NaCl. A cotton stick was used to apply pressure onto one side of the GO leaf to direct salt crystallization in the opposite direction.

### 3 RESULTS & DISCUSSION

#### 3.1 Water Transport

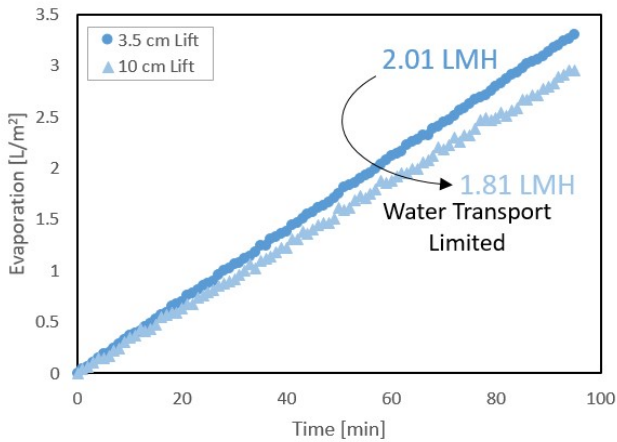


Figure 3: Evaporation under varying capillary lift conditions

The effects of water lift on the evaporation flux were determined by monitoring the evaporation rate of two solutions at different water level heights in the GO setup: (1) 3.5 cm below the GO leaf and (2) 10.0 cm below the GO leaf. The resulting evaporation fluxes were 2.02 L per m<sup>2</sup> per hr (LMH), and 1.81 LMH, respectively (see Fig. 3). Modeling the capillaries of the water transporter as a cylindrical tubes, the passive water flux can be predicted by relating capillary forces to gravitational forces and applying them to Hagen-Poiseuille flow:

$$J_w = \frac{d^2}{32\mu} \left( \frac{4\sigma\cos\alpha}{dh} - \rho g \right) \quad (1)$$

where  $d$  is the diameter of the capillary,  $\mu$  is the viscosity of water,  $\sigma$  is the surface tension of water,  $\alpha$  is contact angle,  $h$  is the water lifting height,  $\rho$  is the density of water, and  $g$  is the gravitation acceleration. It should be noted that the effects of tortuosity and porosity were neglected. By applying equation 1 for the flux rate in the water transport limited regime ( $h = 10$  cm), a hypothetical capillary diameter of 0.30 mm of the water transporter was calculated. This hypothetical diameter can serve as a parameter when comparing various water transporting

materials. However, to develop a more accurate comparison parameters, the model should be updated to better represent flow through the water transporting material. Although, Hagen-Poiseuille flow has served as a starting place for this model, modeling the water transporter as a cylindrical capillary may be a poor assumption. Other flow models are currently being investigated.

#### 3.2 Salt Crystallization

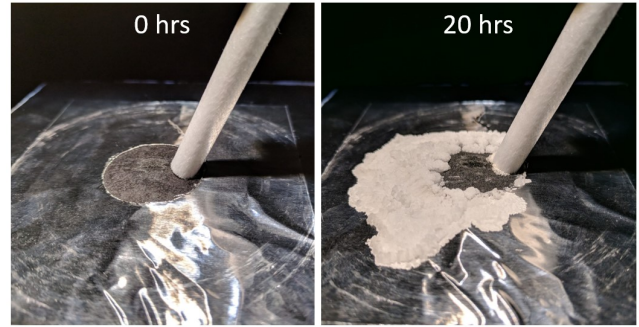


Figure 4: Controlled crystallization of NaCl on the GO Leaf

To control crystal formation of NaCl, a cotton stick was placed on the surface of the GO leaf in order to apply pressure to the material surface. After 20 hours, salt crystals appeared to form in the opposite direction of the applied pressure. These crystals even extended beyond the confines of the GO leaf area to form on nearby surfaces. This behavior was likely caused by preferential flow patterns from the water transporter and the GO leaf. In the region where pressure was applied, the rate of water replenishment was greater than the rate of crystallization, inhibiting salt crystal growth. However, in regions away from where pressure was applied, the rate of water replenishment was slower than salt crystallization. The ability of the salt crystals to extend beyond the area of the GO leaf indicates that the salt itself is capable of transporting water. This is in agreement with observations that the salt crystals appeared to be saturated with water. Therefore, it is hypothesized that the salt crystallization is capable of increasing the rate of evaporation by increasing the surface area from which evaporation can take place.

### 4 FUTURE OUTLOOK

Solar desalination through steam generation has great potential. However, the technology development is still in its infancy. This research has begun to analyze some of the technical challenges associated with passive water transport and salt crystallization. Building on the models discussed in this paper, the properties and water lifting potential of an ideal water transporter will be identified. Furthermore, being able to control the direction salt crystal formation may not just prevent degraded performance when operating on saline water sources, but enhance it by increasing the surface area available for evaporation. Through the

continued research of the technical aspects surrounding steam-generating materials, the true potential of solar desalination technology can begin to be evaluated and its competitive advantage in specific applications discerned.

## REFERENCES

- [1] Elimelech, Menachem, and William A. Phillip. "The future of seawater desalination: energy, technology, and the environment." *Science* 333.6043 (2011): 712-717.
- [2] V.G. Gude, N.N. Khandan and S. Deng. "Renewable and sustainable approaches for desalination." *Renew. Sustain. Energy Rev.*, 14 (2010) 2641-2654.
- [3] Lazarova, Valentina, Kwang-Ho Choo, and Peter Cornel, eds. *Water-energy interactions in water reuse*. IWA publishing, 2012.
- [4] Memon, Fayyaz Ali, and Sarah Ward, eds. *Alternative water supply systems*. IWA Publishing, 2014.
- [5] Tong, Tiezheng, and Menachem Elimelech. "The global rise of zero liquid discharge for wastewater management: drivers, technologies, and future directions." *Environmental science & technology* 50.13 (2016): 6846-6855.
- [6] Ghasemi, Hadi, et al. "Solar steam generation by heat localization." *Nature communications* 5 (2014): ncomms5449.
- [7] Bae, Kyuyoung, et al. "Flexible thin-film black gold membranes with ultrabroadband plasmonic nanofocusing for efficient solar vapour generation." *Nature communications* 6 (2015): 10103.
- [8] Zhou, Lin, et al. "Self-assembly of highly efficient, broadband plasmonic absorbers for solar steam generation." *Science advances* 2.4 (2016): e1501227.
- [9] Zhang, Panpan, et al. "Vertically aligned graphene sheets membrane for highly efficient solar thermal generation of clean water." *ACS nano* 11.5 (2017): 5087-5093.
- [10] Finnerty, Casey, et al. "Synthetic Graphene Oxide Leaf for Solar Desalination with Zero Liquid Discharge." *Environmental science & technology* 51.20 (2017): 11701-11709.
- [11] Jiang, Qisheng, et al. "Bilayered biofoam for highly efficient solar steam generation." *Advanced Materials* 28.42 (2016): 9400-9407.
- [12] Liu, He, et al. "High-Performance Solar Steam Device with Layered Channels: Artificial Tree with a Reversed Design." *Advanced Energy Materials* (2017).
- [13] Ni, George Wei, et al. "A Salt-Rejecting Floating Solar Still for Low-Cost Desalination." *Energy & Environmental Science*(2018).
- [14] MohammadáSajadi, Seyed, and Sing HiáWang. "A flexible anti-clogging graphite film for scalable solar desalination by heat localization." *Journal of Materials Chemistry A* 5.29 (2017): 15227-15234.
- [15] Wheeler, Tobias D., and Abraham D. Stroock. "The transpiration of water at negative pressures in a synthetic tree." *Nature* 455.7210 (2008): 208.
- [16] Chen, Jing M., and T. A. Black. "Defining leaf area index for non-flat leaves." *Plant, Cell & Environment* 15.4 (1992): 421-429.
- [17] Peduzzi, Alicia, et al. "Estimating leaf area index in intensively managed pine plantations using airborne laser scanner data." *Forest Ecology and Management* 270 (2012): 54-65.
- [18] Lovelock, C. E.; Feller, I. C. Photosynthetic performance and resource utilization of two mangrove species coexisting in a hypersaline scrub forest. *Oecologia* 2003, 134 (4), 455-462.
- [19] Atkinson, M. R., et al. "Salt regulation in the mangroves *Rhizophora mucronata* Lam. and *Aegialitis annulata* Rbr." *Australian Journal of Biological Sciences* 20.3 (1967): 589-600.
- [20] Ye, Shibing, Jiachun Feng, and Peiyi Wu. "Highly elastic graphene oxide–epoxy composite aerogels via simple freeze-drying and subsequent routine curing." *Journal of Materials Chemistry A* 1.10 (2013): 3495-3502.